

In-plane Heterostructures of Graphene and Hexagonal Boron Nitride with Controlled Domain Sizes

Zheng Liu, Lulu Ma, Gang Shi, Wu Zhou, Yongji Gong, Sidong Lei, Xuebei Yang, Jiangnan Zhang, Jingjiang Yu, Ken Hackenberg, Aydin Babakhani, Juan-Carlos Idrobo, Robert Vajtai, Jun Lou, and Pulickel M. Ajayan

1. Random G/h-BN domains

In our previous work, we demonstrated the synthesis of hybridized boron nitride and graphene domains with thickness of a few atomic layers and size of a few nanometer by introduce h-BN and carbon sources simultaneously.¹ The domain size obtained from this approach is too small for individual characterizations. By optimizing the growing conditions, the feature size of G/h-BN domains can be grown more than a few hundreds of micron.

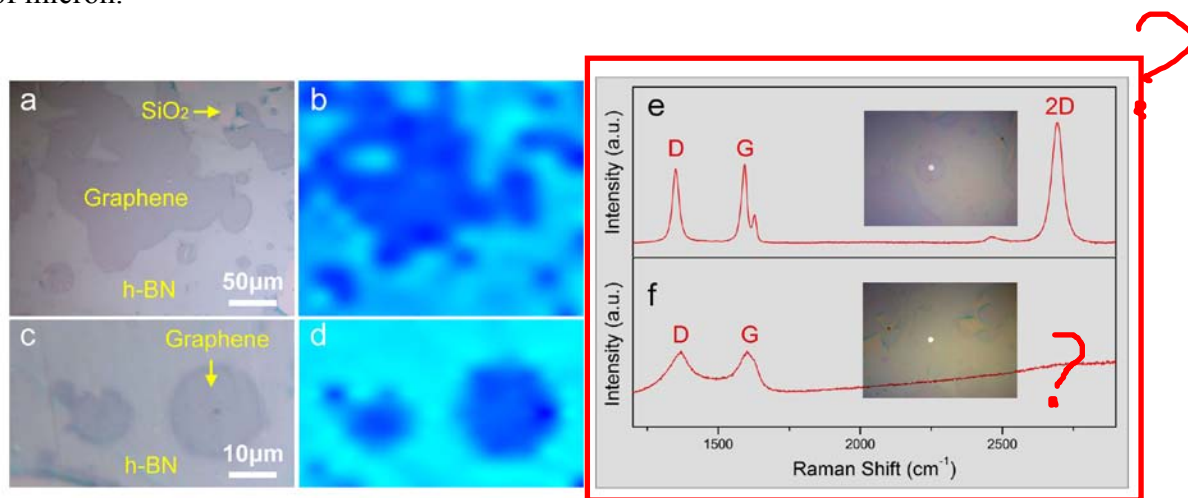


Figure S1. As-transferred random G/h-BN domains on SiO₂ substrate and Raman spectra. (a) and (c) Optical images of the random G/h-BN domains. Graphene areas are in light pink and the rest are h-BN. Some uncovered SiO₂ substrate can also be found, as marked by the arrow. (b) and (d) Corresponding Raman maps at a wavelength of 2700 cm⁻¹. Graphene is shown in blue, and h-BN in green. (e) and (f) Raman spectra of random graphene and h-BN regions, respectively, as shown in the insets. The white dots indicate the location where the spectra were acquired.

The domain size of the patterns ranges from a few to hundred microns with various shapes. The typical Raman spectra, shown in Figs. S1e and S1f, were taken from random graphene and h-BN regions with a laser wavelength of 514 nm. The graphene spectrum corresponds to a few-layered film. The D and D' peaks indicate that the concurrent-growth of graphene and h-BN would induce more defects than the pristine CVD graphene. For the Raman spectra from h-BN, one can clearly see the photoluminescence in whole spectrum background induced by the h-BN layers. It is well confirmed by our previous work that the Raman peaks of the h-BNC film were induced by the hybridized graphene and h-BN domains together, which show a mixed broad D band at 1360 cm^{-1} . The graphene and h-BN regions can be easily differentiated in the Raman mapping (Fig. S1b and S1d).

2. SEM and AFM characterizations of shape engineered G/h-BN

Figure S2 shows SEM images of various G/h-BN in-plane structures on SiO_2 , including stripes, triangles and squares. G/h-BN stripes with millimeter size ($2.3\text{ mm} \times 2.3\text{ mm}$) are shown in Fig. S2a. The top-right region was broken during transfer. We noticed that the film was not broken along the direction of the stripe (Fig. S2b), demonstrating a strong bonding between graphene and h-BN. The widths of graphene strips are $\sim 8\text{ }\mu\text{m}$ and h-BN stripes are $\sim 12\text{ }\mu\text{m}$. Figures 2c and 2d are SEM images of a G/h-BN triangle array. The side lengths of the triangles are $\sim 40\text{ }\mu\text{m}$. SEM images of G/h-BN square array are shown in Figs. 2e and 2f. The side lengths of the squares are also $\sim 40\text{ }\mu\text{m}$. The light regions are graphene and the rest are h-BN for all samples. The dielectric SiO_2 substrate and the ultrathin layers caused the low contrast measured in the images.

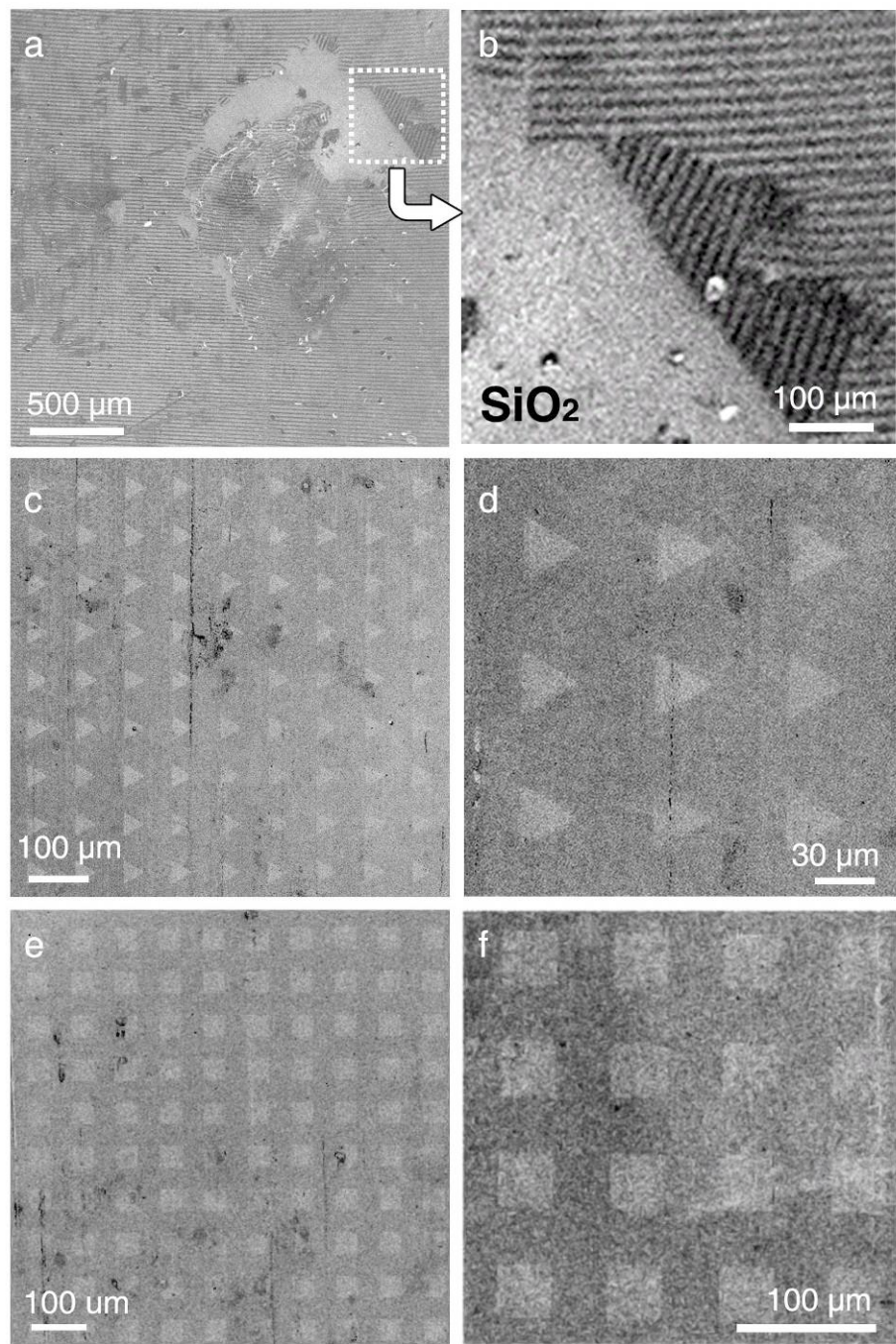


Figure S2. SEM images of as-transferred G/h-BN patterns. (a) and (b) SEM images of alternative graphene/h-BN stripes. The white arrow in Fig. S2a indicates a peel-off G/h-BN region. (c) and (d) SEM images of graphene triangles imbedded in h-BN. (e) and (f) SEM images of graphene squares and h-BN.

AFM images were acquired from the G/h-BN samples in order to determine the thicknesses and electrical response of the samples at various locations. Figures S3a and S3b are height topography of the graphene and h-BN regions, respectively. The thicknesses of graphene and h-BN layers can be well controlled under 2 nm.

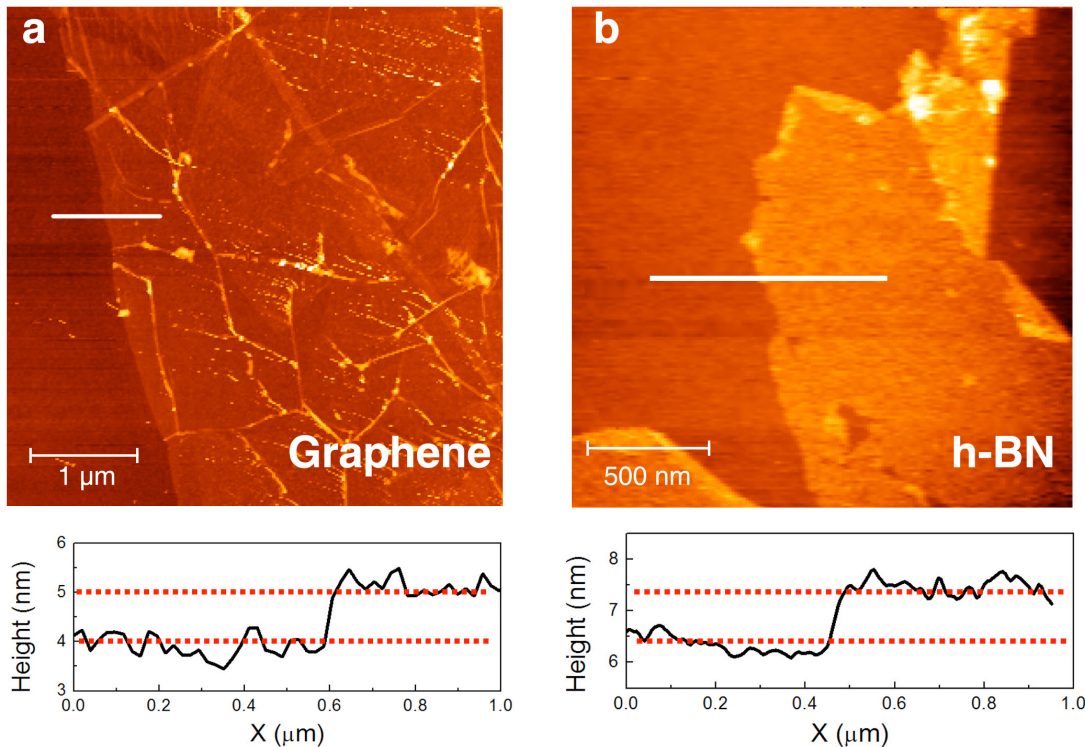


Figure S3. AFM images of the G/h-BN films. (a) Topography of graphene region showing a thickness of ~ 1 nm. (b) Topography of h-BN region showing a thickness of ~ 1 nm in h-BN regions.

3. G/h-BN nano-architectures via the assist of focus ion beam (FIB) etching

To obtain a smaller feature size for the patterned G/h-BN heterostructures, we employed FIB to etch the h-BN directly. We demonstrate that the feature size of G/h-BN shapes can be down to 100 nm, as shown in Fig. S4. The current density of ion beam is 40 pA. The dotting array (Fig. S4a) and lines (Fig. S4c) have been etched by FIB. The diameter of the dots is 500 nm. The width of the lines is 2 μ m, 1 μ m, 500 nm and 200 nm, respectively. The etched h-BN samples will be transferred to CVD furnace for the growth of graphene. Fig. S4b and S4d are corresponding Raman maps of G/h-BN patterns after the growth of

graphene using the graphene 2D Raman peak. The green regions are graphene and blue are h-BN. The spatial resolution of the Raman map is limited by the diffraction limit.

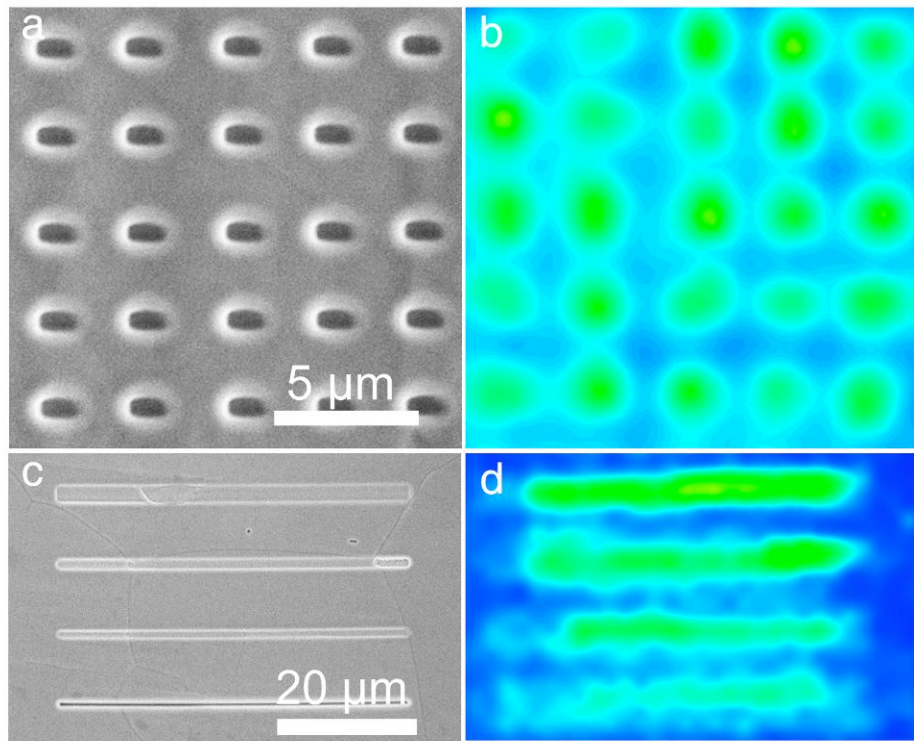


Figure S4. Shape engineering of G/h-BN patterns by FIB etching. (a) and (c) SEM images of h-BN films on Cu foils after etching with different patterns. The diameter of dots in (a) is 500nm. (b)-(d) Raman maps the G/h-BN patterns using the graphene 2D band.

4. STEM imaging and chemical analysis of h-BN domains and the G/h-BN interface

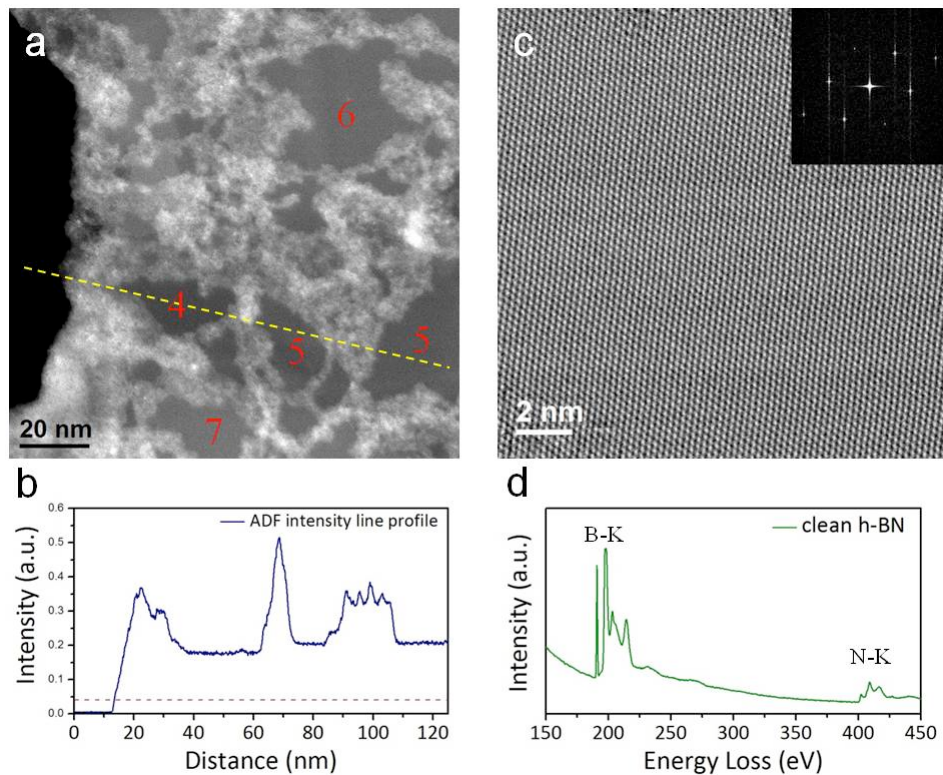


Figure S5. STEM characterization of the h-BN domains in the G/h-BN heterostructure. (a) STEM-ADF from a region inside the h-BN film, away from the G/h-BN interface. Part of the film was broken during the TEM sample preparation, leaving a hole on the left side of the image. The bright stripes in the image are polymer residuals, while some regions of the h-BN film display clean surface without polymer residual. (b) Intensity line profile of the ADF image, along the highlight trajectory shown in Figure a. The image intensity can be used to quantify the thickness of the h-BN film, since the intensity of the ADF image for thin layered materials is roughly proportional to the number of layers. The dash line marks the intensity from monolayer h-BN. The number of BN layers in different regions of the h-BN film is indicated in Figure a. (c) STEM-BF image from a clean region of the h-BN film without contamination. Inset: FFT of the image showing the hexagonal structure of the film. (d) EELS acquired from the clean region of the h-BN film showing the absence of carbon (the carbon K-edge is located 281 eV). This confirms the formation of lateral h-BN/graphene hetero-structure (*i.e.* the subsequently grown graphene does not grow on top of the h-BN domains).

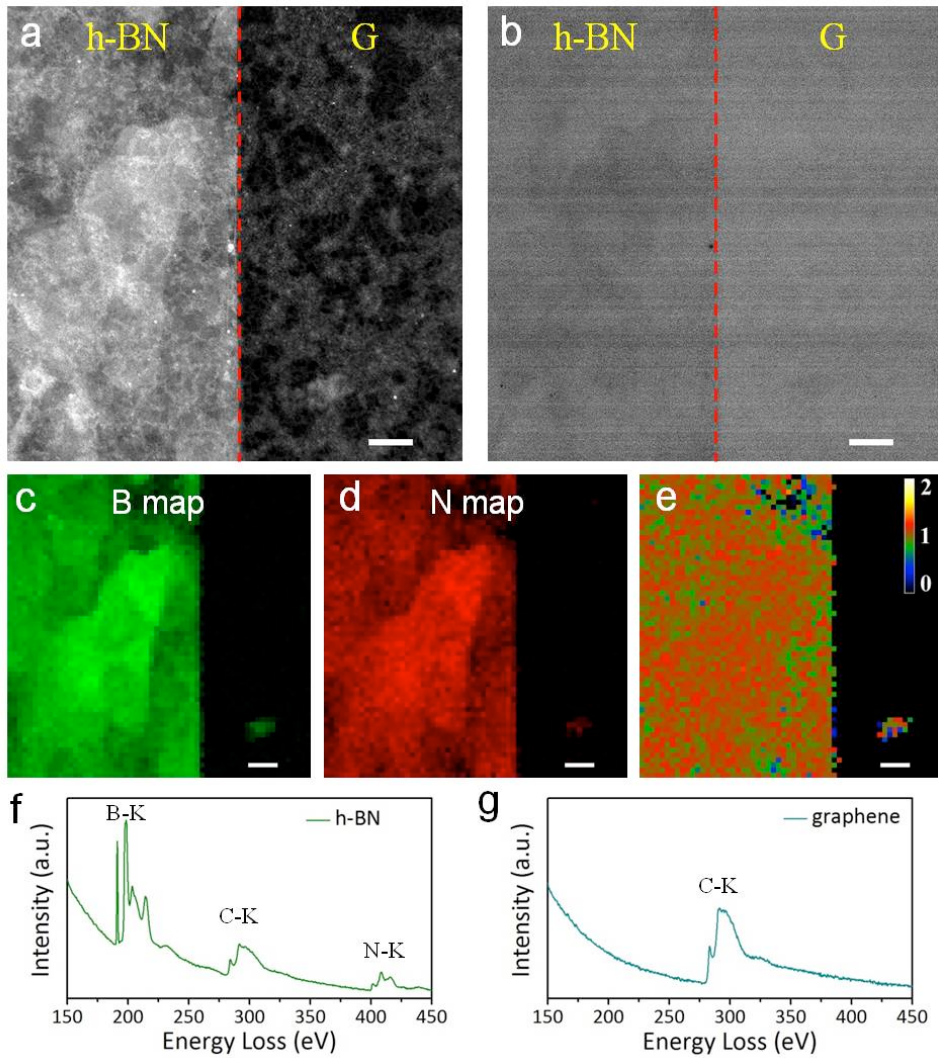


Figure S6. Chemical mapping of h-BN/graphene interface. (a, b) Simultaneous acquired STEM ADF (a) and BF (b) images showing the presence of the h-BN/graphene interface. The bright contrast in Figure A in the graphene region comes from the polymer residuals and hydrocarbon contaminations during the TEM sample preparation. The regions with the lowest contrast in the graphene layer are exposed graphene without polymer residuals. (c, d) Boron and nitrogen maps from the whole area shown in Figure A. Sharp interface between the h-BN and graphene layers can be clearly seen from the B and N maps. (e) N/B atomic ratio map. The average N/B ratio from the whole mapping area is 1.1 ± 0.1 . (f, g) EEL spectra extracted from the h-BN side and the graphene side. The carbon signal from the BN side is mostly from the polymer residuals on the BN surface and hydrocarbon contaminations. Scale bars: 50 nm.

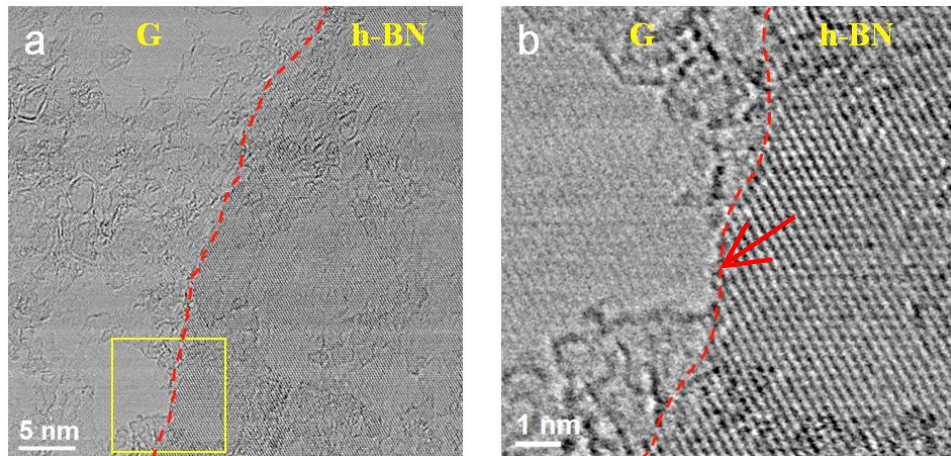


Figure S7. STEM bright field imaging of the h-BN/graphene interface. Figure S7b is a magnified view of the highlighted region in A. The positions of the interfaces are marked by the red dashes. The presence of polymer residuals makes it difficult to resolve the atomic structure at the G/h-BN interface. However, from the clean region of the interface (highlighted by the arrow in Figure S7b), it can be clearly observed that the lattice fringes from both graphene and h-BN extend to the interface, forming seamless integration at the interface without any gap.

5. Comparison for XPS data of in-plane and vertically stacked G/h-BN

To further confirm the in-plane growth of graphene and h-BN layers, depth profile XPS was performed at the G/h-BN interface region (Figure S8). The results are compared with those of h-BN-on-G stacks we have studied before.² XPS depth profile provides information about the elemental distribution in Z direction of the sample, via alternatively sputtering the sample layer-by-layer and collecting XPS spectra. High-energy Ar ion-beam (accelerated voltage is 3KV) was used to sputter a G/h-BN strip sample (Fig. S2a).

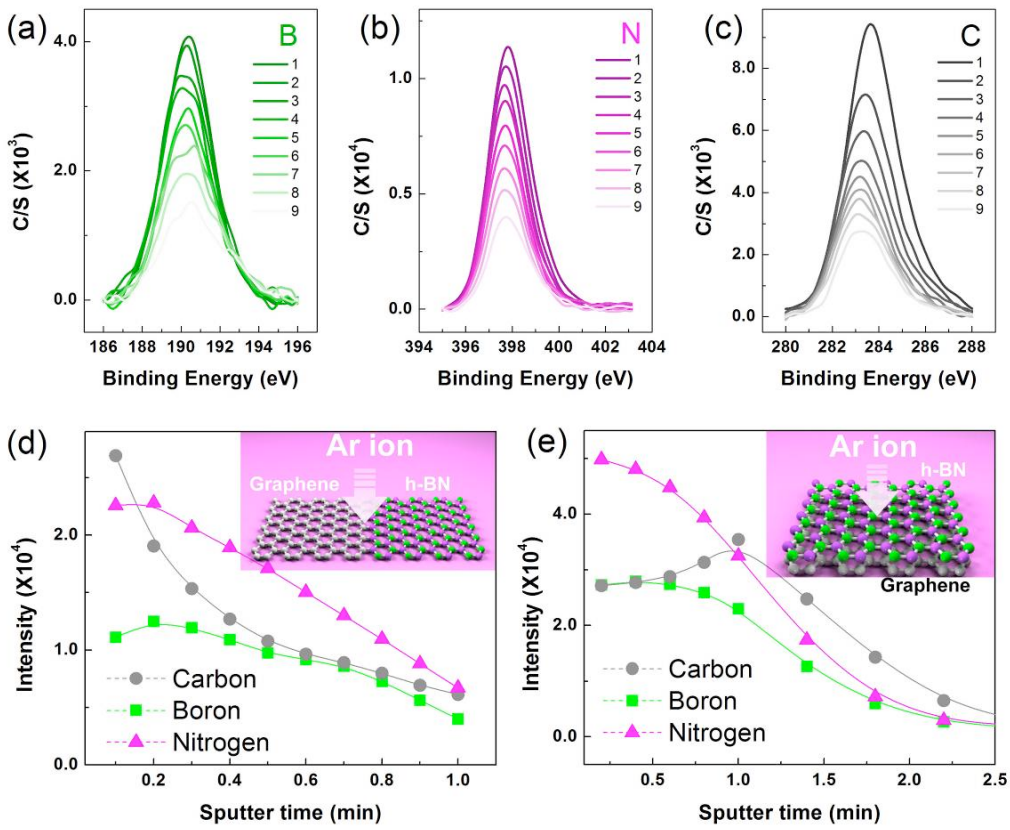


Figure S8. XPS depth profile of G/h-BN in-plane heterostructure vertical stacks. (a) – (c) XPS spectra of Boron, Nitrogen and Carbon (from 1 to 9, in order) of in-plane G/h-BN patterns during Ar-ion etching in 1 min. (d) and (e) Intensity evolution of the C, B, and N signals as a function of the sputter time for the G/h-BN in-plane pattern and the G/h-BN vertical stack during etching. Inset: Illustrations of the in-plane and vertical configurations of graphene and h-BN.

For the boron and nitrogen spectra (Fig. S8a and S8b), their 1s peaks are located at 189.6 ~ 190.7 eV and 397.7 ~ 397.8 eV, respectively, which is close to the value of bulk boron nitride with hexagonal phase that was reported previously.^{3,4} For graphene (Fig. S8c), the C 1s peaks locate at 283.0 ~ 283.6 eV, corresponding to the value (284.5 eV) in graphene.⁵ For all B, N and C, sputtering process will etch these atoms away layer-by-layer, and therefore result in a gradual decrease of the signals. The intensity versus sputtering time for B, N and C are shown in Fig. S8d and S8e. For G/h-BN in-plain patterns, the intensity for all B, N and C decrease monotonically and finally close to zero. However, for the vertically stacked G/h-BN structure (Fig. S8e), the intensity of carbon slightly increases at the first few sputtering processes due to the removal of the top BN

layers, and then decreases when part of the graphene layer starts to be etched away. These results match the architectures of the two samples, *i.e.* the in-plane and stacked heterostructures (insets in Fig. S8d and S8e), respectively.

6. RF measurements of various graphene/h-BN devices.

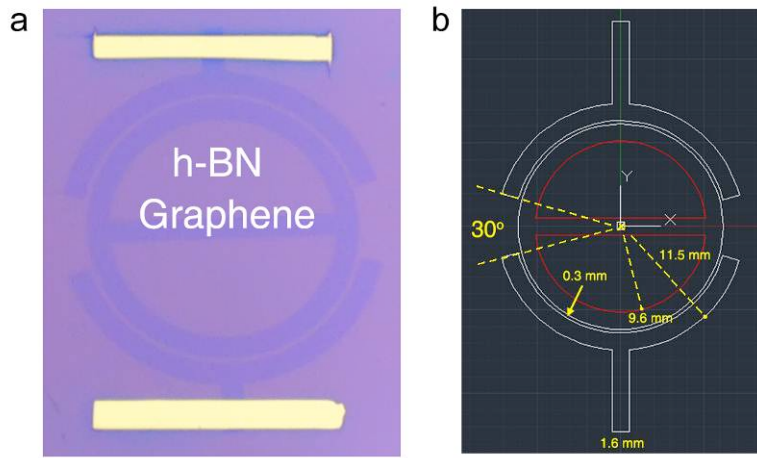


Figure S9. Geometries of G/h-BN split closed-loop resonator for serial RLC circuit modeling. (a) Optical image. (b) Dimensions and geometry parameters. The stripe width of graphene is ~ 1.6 mm and the radius of the ring is ~ 11.5 mm, the gap between input/output lines and the ring resonator is 0.3 mm, and the opening angle of input/output coupling is 30°

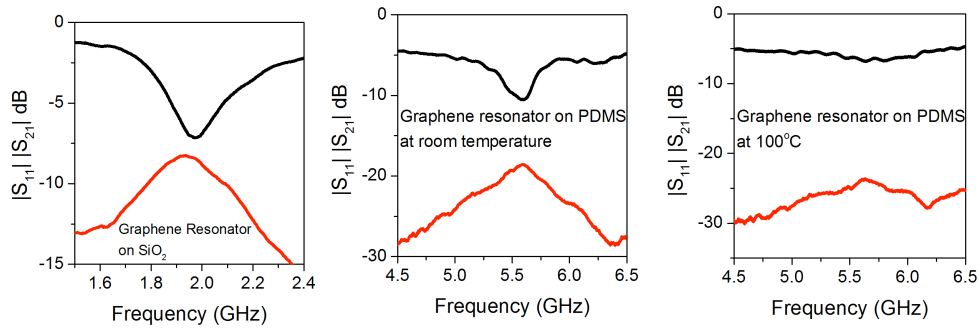


Figure S10. RF measurements of Graphene split closed-loop resonator fabricated on SiO_2 and PDMS. (a) RF performance of graphene resonator on SiO_2 . (b-c) RF performance of graphene resonator on PDMS at room temperature and 100°C . Direct fabrications of graphene on PDMS will result to the poor performance devices. Comparable with the device on SiO_2 , Such device won't work at a temperature above 100°C due to the poor thermal stabilities of PDMS (see Figure S11). The experiments were performed in air.

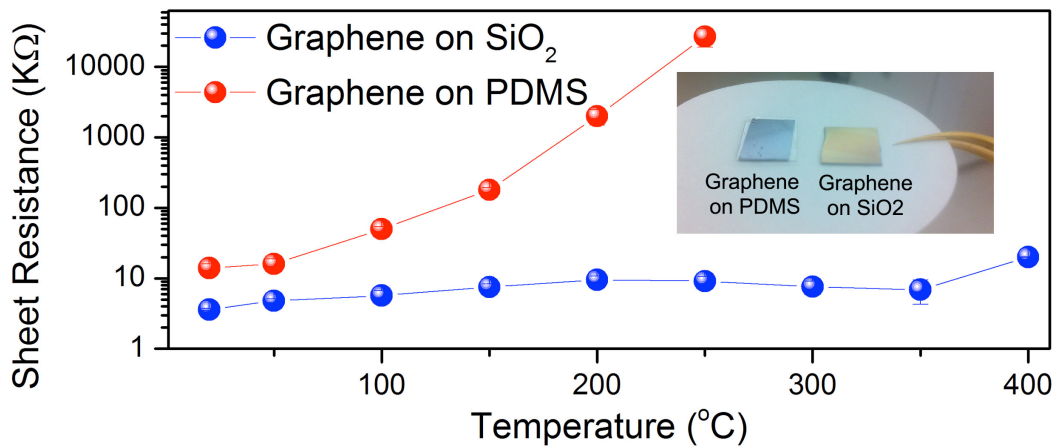


Figure S11. Comparison of temperature dependency of the graphene sheet resistance using SiO₂ and PMDS as substrates. Red: With PDMS as a substrate, graphene sheet resistance exponentially increases by temperature. Blue: While on SiO₂, graphene will retain a low sheet resistance without obvious variation up to 400°C. Inset: Photos of graphene on PDMS and SiO₂. The experiments were performed in air.

References:

1. Ci, L., et al. Atomic layers of hybridized boron nitride and graphene domains. *Nat Mater* **2010**, *9*, 430-435.
2. Liu, Z.; Song, L.; Zhao, S.; Huang, J.; Ma, L.; Zhang, J.; Lou, J.; Ajayan, P. M. Direct Growth of Graphene/Hexagonal Boron Nitride Stacked Layers. *Nano Lett.* **2011**, *11*, 2032-2037.
3. Moulder, J.; Stickle, W.; Sobol, P., *Handbook of X Ray Photoelectron Spectroscopy (P/N 624755)*. Perkin-Elmer, Physical Electronics Division: 1992.
4. Park, K. S.; Lee, D. Y.; Kim, K. J.; Moon, D. W. Observation of a hexagonal BN surface layer on the cubic BN film grown by dual ion beam sputter deposition. *Applied Physics Letters* **1997**, *70*, 315-317.
5. Sun, Z.; Yan, Z.; Yao, J.; Beitler, E.; Zhu, Y.; Tour, J. M. Growth of graphene from solid carbon sources. *Nature* **2010**, *468*, 549-552.